

## Boronic Acid-Based Bipyridinium Salts as Tunable Receptors for Monosaccharides and $\alpha$ -Hydroxycarboxylates

Soya Gamsey, Aaron Miller, Marilyn M. Olmstead,<sup>†</sup> Christine M. Beavers,<sup>†</sup> Lacie C. Hirayama, Sulolit Pradhan, Ritchie A. Wessling, and Bakthan Singaram\*

Department of Chemistry and Biochemistry, University of California, Santa Cruz, California 95064, and Department of Chemistry, University of California, Davis, California 95616

Received September 11, 2006; E-mail: singaram@chemistry.ucsc.edu

**Abstract:** Several novel diboronic acid-substituted bipyridinium salts were prepared and, using a fluorescent reporter dye, were tested for their ability to selectively bind various monosaccharides and  $\alpha$ -hydroxycarboxylates in an aqueous medium. The fluorescence sensing mechanism relies on the formation of a ground-state charge-transfer complex between the dye and bipyridinium. An X-ray crystal structure of this complex is described herein. Glucose selectivity over fructose and galactose was achieved by designing the bipyridinium-based receptors to be capable of attaining a 1:1 receptor/substrate stoichiometry via cooperative diboronic acid binding.

Boronic acids are known to reversibly bind diols with high affinity to form cyclic esters.<sup>1</sup> As a result, many boronic acid-containing molecules have been utilized as chemosensors for the recognition of carbohydrates.<sup>2</sup> Specifically, there has been much interest focused on the design of boronic acid-containing fluorescent glucose sensors that operate under physiological conditions.<sup>3</sup> If optimized, such sensors can be implantable, and used to continuously monitor glucose concentrations in preterm infants,<sup>4</sup> patients in the Intensive Care Unit,<sup>5</sup> and in people suffering from diabetes.<sup>6</sup>

In order to develop a successful in vivo boronic acid-based glucose sensor, an important criterion that must be met is the preferential binding of glucose over other physiologically significant monosaccharides such as fructose. This is a challenging objective since phenylboronic acids display a higher binding affinity for fructose.<sup>7</sup> To increase glucose selectivity,

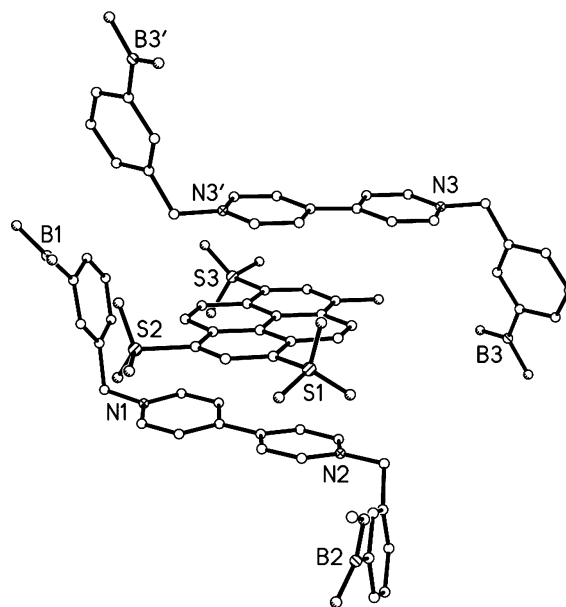


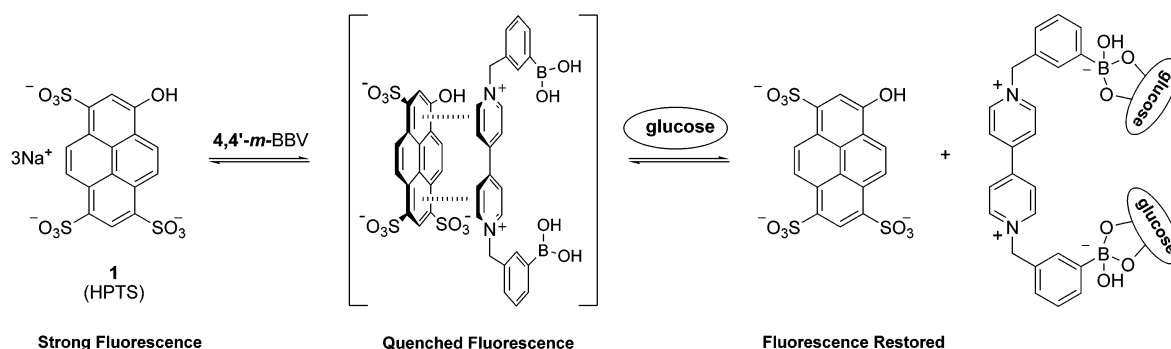
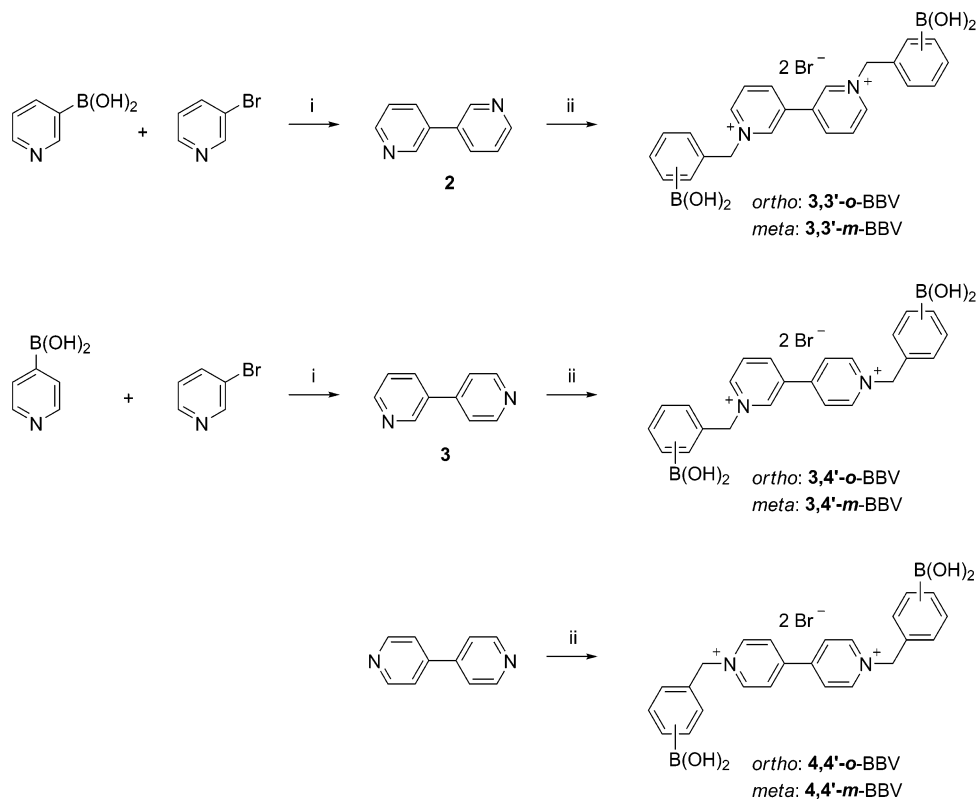
**Figure 1.** Portion of the structure of  $(4,4'\text{-}m\text{-BBV}^{2+})_3(\text{HPTS}^{3-})_2$ . The  $\text{BBV}^{2+}$  molecule containing N1 and N2 has no crystallographic symmetry, whereas the top molecule, containing N3, has crystallographic inversion symmetry. The  $\text{HPTS}^{3-}$  species lies between these two cations with the sulfonate groups staggered with respect to the basic  $\pi$ -stacking motif.

the concept of bidentate binding via diboronic acids has been utilized.<sup>8</sup> In this approach, the sensor molecule contains two arylboronic acid moieties spatially disposed in a way that allows for cooperative binding to a single glucose molecule. For a given

<sup>†</sup> Department of Chemistry, University of California at Davis.

- (1) (a) Lorand, J. P.; Edwards, J. O. *J. Org. Chem.* **1959**, *24*, 769–774. (b) Kuivila, H. G.; Keough, A. H.; Soboczenski, E. J. *J. Org. Chem.* **1954**, *19*, 780–783. (c) Sugihara, J. M.; Bowman, C. M. *J. Am. Chem. Soc.* **1958**, *80*, 2443–2446.
- (2) For reviews see: (a) Wang, W.; Gao, X.; Wang, B. *Curr. Org. Chem.* **2002**, *6*, 1285–1317. (b) Striegler, S. *Curr. Org. Chem.* **2003**, *7*, 81–102. (c) James, T. D.; Shinkai, S. *Top. Curr. Chem.* **2002**, *218*, 159–200.
- (3) (a) Czarnik, A. W. *Fluorescent Chemosensors for Ion and Molecule Recognition*; American Chemical Society: Washington, DC, 1993; Vol. 538. (b) Fang, H.; Kaur, G.; Wang, B. *J. Fluoresc.* **2004**, *14*, 481–489. (c) Cao, H.; Heagy, M. D. *J. Fluoresc.* **2004**, *14*, 569–584. (d) Pickup, J. C.; Hussain, F.; Evans, N. D.; Rolinski, O. J.; Birch, D. J. *Sens. Bioelectron.* **2005**, *20*, 2555–2565.
- (4) Cornblath, M.; Reisner, S. H. *N. Engl. J. Med.* **1965**, *273*, 378–381.
- (5) (a) Van den Berghe, G. *Int. J. Obes.* **2002**, *26*, S3–S8. (b) Van den Berghe, G.; Wilmer, A.; Hermans, G.; Meersseman, W.; Wouters, P. J.; Milants, I.; Van Wijngaerden, E.; Bobbaers, H.; Bouillon, R. *N. Engl. J. Med.* **2006**, *354*, 449–461. (c) Finney, S. J.; Zekveld, C.; Elia, A.; Evans, T. W. *J. Am. Med. Assoc.* **2003**, *290*, 2041–2047.
- (6) (a) Wentholt, I. M.; Vollebregt, M. A.; Hart, A. A.; Hoekstra, J. B.; DeVries, J. H. *Diabetes Care* **2005**, *28*, 2871–2876. (b) Wilson, Darrell, M.; Block, J. *Diabetes Technol. Ther.* **2005**, *7*, 788–791. (c) Heinemann, L.; Schmelzeisen-Redeker, G. *Diabetologia* **1998**, *41*, 848–854. (d) Kerr, D. *Int. J. Clin. Pract.* **2001**, *43*–46. (e) Garg, S. K.; Hoff, H. K.; Chase, H. P. *Endocrinol. Metab. Clin. North Am.* **2004**, *33*, 163–173.
- (7) Springsteen, G.; Wang, B. *Tetrahedron* **2002**, *58*, 5291–5300.

- (8) (a) Tsukagoshi, K.; Shinkai, S. *J. Org. Chem.* **1991**, *56*, 4089–4091. (b) Shiomi, Y.; Saisho, M.; Tsukagoshi, K.; Shinkai, S. *J. Chem. Soc., Perkin Trans. 1* **1993**, 2111–2117. (c) James, T. D.; Sandanayake, K. R. A. S.; Shinkai, S. *Angew. Chem., Int. Ed. Engl.* **1994**, *106*, 2287–2289. (d) Eggert, H.; Frederiksen, J.; Morin, C.; Norrild, J. C. *J. Am. Chem. Soc.* **1999**, *64*, 3846–3852. (e) Yang, W.; He, H.; Drueckhammer, D. G. *Angew. Chem., Int. Ed.* **2001**, *40*, 1714–1718. Arimori, S.; Ward, C. J.; James, T. D. *Tetrahedron Lett.* **2002**, *43*, 303–305.

**Scheme 1.** Proposed Glucose-Sensing Mechanism

**Scheme 2.** Boronic Acid-Based Bipyridinium Salts for Analyte Recognition<sup>a</sup>


<sup>a</sup> Reagents and conditions: (i)  $\text{Pd}(\text{OAc})_2$ ,  $\text{PPh}_3$ ,  $\text{Na}_2\text{CO}_3$ , *p*-dioxane, 95 °C, 4 h, 64% (**2**), 70% (**3**); (ii) 2- or 3-bromomethylphenylboronic acid (2.5 equiv), DMF, 70 °C, 48 h, 80% (**3,3'-o-**), 76% (**3,3'-m-**), 77% (**3,4'-o-**), 76% (**3,4'-m-**).

diboronic acid-containing scaffold, the spacing between the boronic acids could be adjusted through synthetic modifications in order to create a glucose-specific binding pocket. However, in many systems, the boronic acids are covalently linked to a reporter (a fluorophore or chromophore),<sup>2</sup> and such modifications to the receptor can prove difficult or impossible to achieve without altering the photophysical properties of the reporter as well.

This problem can be avoided by employing a modular approach to sensor design, where the receptor and the reporter moieties exist as covalently discrete entities. To this end, our laboratory has developed a two-component sensing system comprising a fluorescent dye that serves as the reporter unit and a diboronic acid-containing molecule that acts dually as a fluorescence quencher and a saccharide receptor.<sup>9</sup> We report herein that tuning the receptor unit by synthetically manipulating the spacing between the diboronic acids provides greatly

enhanced glucose selectivity and sensitivity. The different receptors were studied in terms of analyte selectivity (monosaccharides and  $\alpha$ -hydroxycarboxylates), quenching strengths, and reduction potentials.

## Results and Discussion

The sensing ensemble is composed of the anionic fluorescent dye, 8-hydroxypyrene-1,3,6-trisulfonic acid trisodium salt (HPTS,

- (9) (a) Camara, J. N.; Suri, J. T.; Cappuccio, F. E.; Wessling, R. A.; Singaram, B. *Tetrahedron Lett.* **2002**, 43, 1139–1141. (b) Suri, J. T.; Cordes, D. B.; Cappuccio, F. E.; Wessling, R. A.; Singaram, B. *Langmuir* **2003**, 19, 5145–5152. (c) Suri, J. T.; Cordes, D. B.; Cappuccio, F. E.; Wessling, R. A.; Singaram, B. *Angew. Chem., Int. Ed.* **2003**, 42, 5857–5859. (d) Cappuccio, F. E.; Suri, J. T.; Cordes, D. B.; Wessling, R. A.; Singaram, B. *J. Fluoresc.* **2004**, 14, 521–533. (e) Cordes, D. B.; Gamsey, S.; Sharrett, Z.; Miller, A.; Thoniyot, P.; Wessling, R. A.; Singaram, B. *Langmuir* **2005**, 21, 6540–6547. (f) Cordes, D. B.; Miller, A.; Gamsey, S.; Sharrett, Z.; Thoniyot, P.; Wessling, R.; Singaram, B. *Org. Biomol. Chem.* **2005**, 3, 1708–1713. (g) Gamsey, S.; Baxter, N. A.; Sharrett, Z.; Cordes, D. B.; Olmstead, M. M.; Wessling, R. A.; Singaram, B. *Tetrahedron* **2006**, 62, 6321–6331.

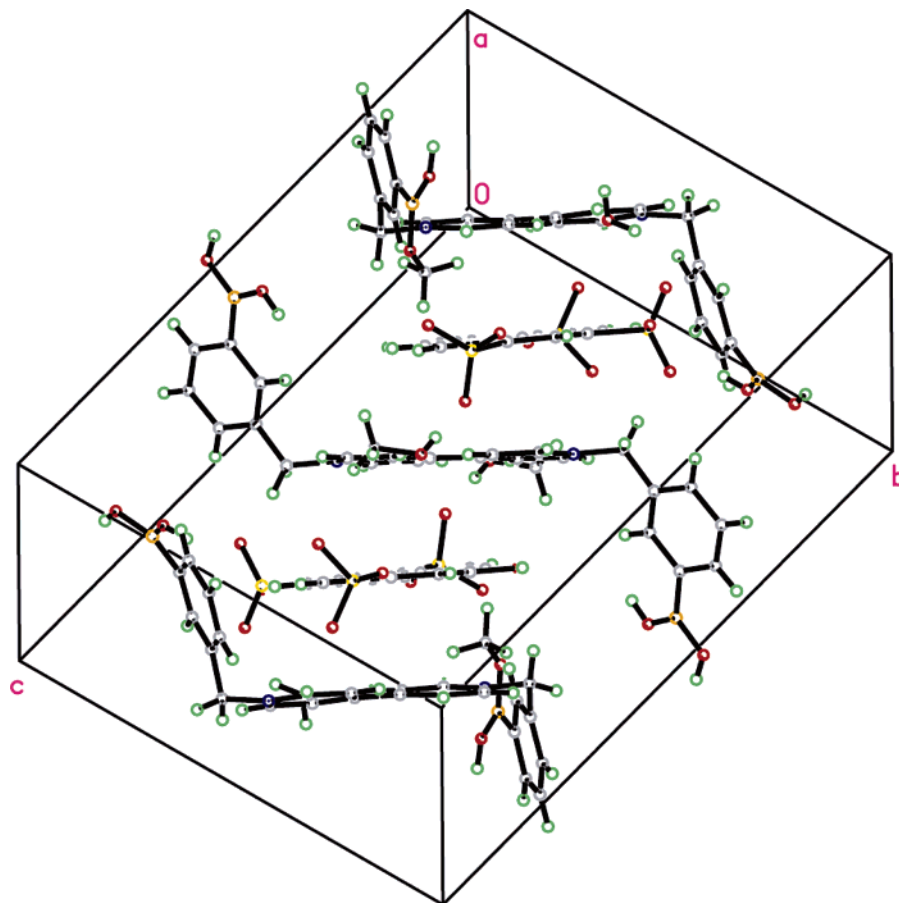


**Figure 2.** View of the unit cell contents of  $(\text{BBV}^{2+})_3(\text{HPTS}^{3-})_2$  showing the donor–acceptor  $\pi$ -stacking arrangement of the molecules edge-on. Solvate methanol and water molecules are omitted for clarity.

1), and a boronic acid-appended viologen,<sup>10</sup> such as **4,4'-m**-BBV (Scheme 1). It is postulated that Coulombic attraction between **1** and **4,4'-m**-BBV results in the formation of a ground-state complex which facilitates electron transfer from the dye to the viologen, leading to a decrease in the fluorescence intensity of the dye. When glucose is added to the system, the boronic acids are converted to tetrahedral anionic glucoboronate esters, which effectively neutralize the cationic viologen, thus greatly diminishing its quenching efficiency, and an increase in fluorescence intensity is observed. To help substantiate the putative glucose-induced dissociation mechanism of the dye and receptor, we have used <sup>11</sup>B NMR to monitor the change in charge of boron from neutral ( $\text{sp}^2$ ) to anionic ( $\text{sp}^3$ ) upon addition of glucose at pH 7.4.<sup>9g</sup>

Several instances of viologens serving as fluorescence quenchers for organic dyes,<sup>11</sup> porphyrins,<sup>12</sup> and polymers<sup>13</sup> have

been reported. Due to their electron-deficient nature, viologens function as acceptors in many charge-transfer (CT) complexes.<sup>14</sup> Baptista and co-workers maintain that HPTS and methyl viologen form a ground-state complex on the basis of UV–vis, fluorescence, and laser flash photolysis studies.<sup>11a</sup> Regarding the initial quenching mechanism in our system, we have proposed, on the basis of UV–vis absorbance studies, that **1** and **4,4'-m**-BBV form a distinct complex.<sup>9e,g</sup> From single-crystal X-ray analysis, we now report the formation of a CT complex in the solid state (Figures 1 and 2).

The asymmetric unit contains one 8-hydroxypyrene-1,3,6-trisulphonate ( $\text{HPTS}^{3-}$ ) molecule, 1.5  $\text{BBV}^{2+}$  molecules, one methanol, and one water molecule. The overall stoichiometry is  $2(\text{HPTS}^{3-}):3(\text{BBV}^{2+})$ . The  $\text{BBV}^{2+}$  molecule that is entirely contained within the asymmetric unit has one boronic acid (B2) that has undergone an esterification with methanol (bottom structure, Figure 1). The dihedral angle between the two pyridine rings of the viologen is  $10.8^\circ$ . The second half of the other

- (10) In general, the term viologen refers to any diquaternized bipyridyl salt.  
 (11) (a) De Borja, E. B.; Amaral, C. L. C.; Politi, M. J.; Villalobos, R.; Baptista, M. S. *Langmuir* **2000**, *16*, 5900–5907. (b) Nakashima, K.; Kido, N. *Photochem. Photobiol.* **1996**, *64*, 296–302. (c) Sun, L.-C.; Yang, Y.-F.; He, J.-J.; Shen, T. *Dyes Pigm.* **1995**, *28*, 275–279. (d) Takenaka, S.; Shigemoto, N.; Kondo, H. *Supramol. Chem.* **1998**, *9*, 47–56.  
 (12) (a) Blondeel, G.; De Keukeleire, D.; Harriman, A.; Milgrom, L. R. *Chem. Phys. Lett.* **1985**, *118*, 77–82. (b) Harriman, A. *Inorg. Chim. Acta* **1984**, *88*, 213–216. (c) Kusumoto, Y.; Watanabe, J.; Kurawaki, J.; Satake, I. *Chem. Lett.* **1987**, 1417–1420. (d) Kusumoto, Y.; Uchikoba, M. *Chem. Lett.* **1991**, 1985–1988. (e) Yanuck, M. D.; Schmehl, R. H. *Chem. Phys. Lett.* **1985**, *122*, 133–138.  
 (13) (a) Chen, L.; McBranch, D. W.; Wang, H.-L.; Helgeson, R.; Wudl, F.; Whitten, D. G. *Proc. Natl. Acad. Sci. U.S.A.* **1999**, *96*, 12287–12292. (b) Gaylord, B. S.; Wang, S.; Heeger, A. J.; Bazan, G. C. *J. Am. Chem. Soc.* **2001**, *123*, 6417–6418. (c) Wang, D.; Wang, J.; Moses, D.; Bazan, G. C.; Heeger, A. J.; Park, J.-H.; Park, Y.-W. *Synth. Met.* **2001**, *119*, 587–588.

- (d) Wang, D.; Wang, J.; Moses, D.; Bazan, G. C.; Heeger, A. J. *Langmuir* **2001**, *17*, 1262–1266. (e) Fan, C.; Hirasa, T.; Plaxco, K. W.; Heeger, A. J. *Langmuir* **2003**, *19*, 3554–3556. (f) Miyashita, T.; Ohsawa, M.; Matsuda, M. *Macromolecules* **1986**, *19*, 585–588.  
 (14) (a) Pia, E.; Toba, R.; Chas, M.; Peinador, C.; Quintela, J. M. *Tetrahedron Lett.* **2006**, *47*, 1953–1956. (b) Monk, P. M. S.; Hodgkinson, N. M.; Partridge, R. D. *Dyes Pigm.* **1999**, *43*, 241–251. (c) Matos, M. S.; Gehlen, M. H. *Spectrochim. Acta, Part A* **1998**, *54A*, 1857–1867. (d) Monk, P. M. S.; Hodgkinson, N. M. *Electrochim. Acta* **1997**, *43*, 245–255. (e) Tsukahara, K.; Kaneko, J.; Miyaji, T.; Abe, K. *Tetrahedron Lett.* **1996**, *37*, 3149–3152. (f) Yoon, K. B. *Chem. Rev.* **1993**, *93*, 321–339. (g) Alvaro, M.; Ferrer, B.; Fornes, V.; Garcia, H. *Chem. Phys. Chem.* **2003**, *4*, 612–617.

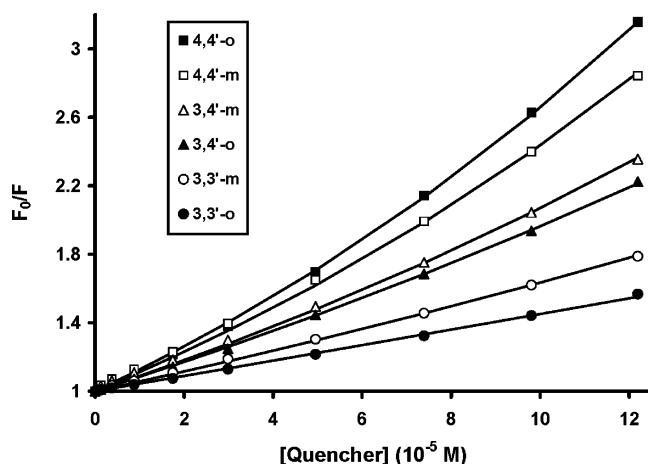


**Figure 3.** Stern–Volmer plot of HPTS ( $4 \times 10^{-6}$  M in pH 7.4 phosphate buffer,  $\lambda_{\text{ex}} = 460$  nm and  $\lambda_{\text{em}} = 510$  nm) with increasing concentrations of BBVs.

**Table 1.** Static ( $K_s$ ) and Dynamic ( $V$ ) Quenching Constants for BBVs with HPTS ( $4 \times 10^{-6}$  M in pH 7.4 Phosphate Buffer,  $\lambda_{\text{ex}} = 460$  nm and  $\lambda_{\text{em}} = 510$  nm)

BBV	$K_s$ ( $\text{M}^{-1}$ )	$V$ ( $\text{M}^{-1}$ )	BBV	$K_s$ ( $\text{M}^{-1}$ )	$V$ ( $\text{M}^{-1}$ )
4,4'-o-	$8900 \pm 200$	$2900 \pm 100$	3,4'-m-	$7500 \pm 200$	$1700 \pm 100$
4,4'-m-	$8100 \pm 100$	$2950 \pm 100$	3,3'-o-	$4300 \pm 200$	$140 \pm 30$
3,4'-o-	$6600 \pm 200$	$1650 \pm 50$	3,3'-m-	$5000 \pm 100$	$700 \pm 50$

BBV<sup>2+</sup> molecule is generated by a center of inversion, giving two coplanar pyridine rings.

The BBV<sup>2+</sup> and HPTS<sup>3-</sup> molecules are arranged in alternating layers that are almost parallel; however, the HPTS<sup>3-</sup> molecule, with three deprotonated sulfonates is too sterically hindered for a perpendicular stacking arrangement (Figure 2). The molecules adopt a slipped stacking motif that permits the distance between the layers to range between 3.25 and 3.46 Å, which is typical for a donor–acceptor CT complex of this type.<sup>15</sup> X-ray structures of CT complexes involving similar viologen acceptors have been reported.<sup>16</sup>

To optimize the system in terms of glucose sensitivity and selectivity, six bipyridinium-based receptors, shown in Scheme 2, were synthesized. The 4,4'-bipyridyl-based receptors (4,4'-o- and 4,4'-m-BBV) have been previously studied and shown to display monosaccharide selectivity of the order fructose  $\gg$  galactose  $>$  glucose.<sup>9g</sup> The relative ratios of the binding constants were parallel to those reported for monoboronic acids which is expected since, for both structures, the intramolecular distance between the two boronic acids is too great to allow for cooperative binding with one glucose molecule. The four other receptors (3,4'-o-, 3,4'-m-, 3,3'-o-, and 3,3'-m-BBV), however, were designed to have shorter intramolecular B–B distances, and therefore each theoretically possesses the ability to form a 1:1 binding scenario with glucose.

Before binding studies were carried out, the quenching characteristics for each of the receptors were established. Figure

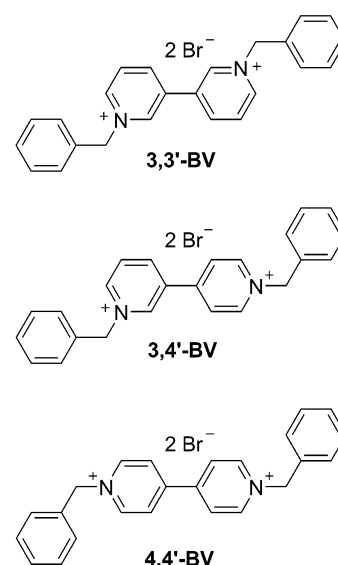


**Figure 4.** Benzyl viologens used in cyclic voltammetry.

**Table 2.** Static ( $K_s$ ) and Dynamic ( $V$ ) Quenching Constants for Benzyl Viologens with HPTS ( $4 \times 10^{-6}$  M in pH 7.4 Phosphate Buffer,  $\lambda_{\text{ex}} = 460$  nm and  $\lambda_{\text{em}} = 510$  nm) and Formal Potentials ( $E^\circ$ ) Measured by CV in pH 7.4 Phosphate Buffer (Scan Rate = 100 mV/s)

	$K_s$ ( $\text{M}^{-1}$ )	$V$ ( $\text{M}^{-1}$ )	$E^\circ$ (mV vs NHE)
4,4'-BV	$15000 \pm 1000$	$2300 \pm 200$	−420
3,4'-BV	$9500 \pm 500$	$2800 \pm 300$	−650
3,3'-BV	$7400 \pm 300$	$2200 \pm 200$	−1100

3 shows a Stern–Volmer plot generated from the fluorescence quenching of HPTS by the receptors. The calculated Stern–Volmer constants,  $K_s$  and  $V$ , indicating the degree of static and dynamic quenching, respectively, are summarized in Table 1. The quenching efficiencies of the viologens were found to be of the order: 4,4'-BBVs  $>$  3,4'-BBVs  $>$  3,3'-BBVs. To help verify our suspicion that these observed differences in quenching behavior are due to the electrochemical properties of the bipyridinium core, cyclic voltammetry studies were carried out on model compounds (benzyl viologens).

We have previously shown that Stern–Volmer quenching constants correlate with association constants, determined by Benesi–Hildebrandt treatment of UV–vis absorbance data, and therefore provide a measure of the strength of the dye–receptor complex.<sup>9b,e</sup> The degree of quenching is also an indication of the electron-accepting abilities of the viologens and should therefore correlate with their reduction potentials.<sup>17</sup> To confirm this relationship, the reduction potentials of benzyl viologens (BV), 4,4'-BV, 3,4'-BV, and 3,3'-BV (Figure 4), were determined by cyclic voltammetry (CV) and were compared to their quenching constants. The Stern–Volmer values for the BVs (Table 2) are higher than those of the boronic-acid containing derivatives,<sup>18</sup> but the quenching trend (4,4'  $>$  3,4'  $>$  3,3') within each series is the same. The measured formal potentials ( $E^\circ$ ) of the BVs correspond with their Stern–Volmer values, in that the  $E^\circ$  values become increasingly more positive with increasing

(15) Yoon, K. B.; Kochi, J. K. *J. Am. Chem. Soc.* **1989**, *111*, 1128–1130.

(16) (a) Kidowaki, M.; Tamaoki, N. *Chem. Commun.* **2003**, 290–291. (b) Yoshikawa, H.; Nishikiori, S.-I. *J. Chem. Soc., Dalton Trans.* **2005**, 3056–3064. (c) Nishikiori, S.-I.; Yoshikawa, H.; Sano, Y.; Iwamoto, T. *Acc. Chem. Res.* **2005**, *38*, 227–234. (d) Yoshikawa, H.; Nishikiori, S.-I.; Ishida, T. *J. Phys. Chem. B* **2003**, *107*, 9261–9267. (e) Willner, I.; Eichen, Y.; Rabinovitz, M.; Hoffman, R.; Cohen, S. *J. Am. Chem. Soc.* **1992**, *114*, 637–644. (f) Sundaresan, T.; Wallwork, S. C. *Acta Crystallogr., Sect. B* **1972**, *28*, 2474–2480. (g) Robinson, P. D.; Smith, K. R.; Vermeulen, L. A. *Acta Crystallogr., Sect. C* **2002**, *C58*, o632–o634.

(17) (a) Amouyal, E.; Zidler, B.; Keller, P.; Moradpour, A. *Chem. Phys. Lett.* **1980**, *74*, 314–317. (b) Keller, P.; Moradpour, A.; Amouyal, E.; Zidler, B. *J. Mol. Catal.* **1981**, *12*, 261–263.

(18) It is proposed that the addition of boronic acids alters the electronics as well as the sterics of the viologens, thereby affecting their static and dynamic quenching constants. See refs 9b,g.



**Table 3.** Apparent Monosaccharide Binding Constants ( $K_b$ ) Determined for the BBVs ( $5 \times 10^{-4}$  M) with HPTS ( $4 \times 10^{-6}$  M in Phosphate Buffer,  $\lambda_{\text{ex}} = 460$  nm and  $\lambda_{\text{em}} = 510$  nm) and Their Monosaccharide Selectivity Ratios

	$K_b$ ( $\text{M}^{-1}$ )			selectivity ratios	
	glucose	galactose	fructose	glu/fru	glu/gal
4,4'- <i>o</i> -	$27 \pm 5$	$37 \pm 5$	$800 \pm 100$	0.03	0.73
4,4'- <i>m</i> -	$14 \pm 5$	$25 \pm 5$	$300 \pm 50$	0.05	0.56
3,4'- <i>o</i> -	$260 \pm 50$	$70 \pm 10$	$800 \pm 100$	0.33	3.7
3,4'- <i>m</i> -	$65 \pm 10$	$35 \pm 5$	$400 \pm 50$	0.16	1.9
3,3'- <i>o</i> -	$1900 \pm 200$	$180 \pm 50$	$1100 \pm 200$	1.7	11
3,3'- <i>m</i> -	$53 \pm 10$	$45 \pm 5$	$500 \pm 50$	0.11	1.2

quenching strength (Table 2). This indicates that the quenching efficiencies (measured by  $K_s$  and  $V$ ) of the viologens are dependent upon their electron-accepting abilities (measured by  $E^\circ$ ). Preliminary CV studies indicate that the boronic acid-containing viologens (BBVs) display a similar trend (data not shown). A detailed investigation of the electrochemical behavior of the BBVs in the presence and absence of various saccharides is currently underway.

The apparent binding affinities of each of the BBVs for glucose were determined by measuring the degree of fluorescence enhancement obtained when increasing amounts of glucose (0–35 mM) were added to an aqueous solution (pH 7.4 phosphate buffer, 0.1 M ionic strength) of **1** ( $4 \times 10^{-6}$  M) and BBV ( $5 \times 10^{-4}$  M).<sup>19</sup> The calculated binding constants ( $K_b$ ) show that 3,3'-*o*-BBV has a binding affinity for glucose several orders of magnitude higher than the other BBVs (Table 3). Further inspection of the binding constants reveals a general trend, in which the ortho-substituted bipyridyls have higher affinities than their corresponding meta-derivatives. Most likely, this is due to an intramolecular B  $\rightarrow$  N charge interaction, previously described,<sup>9b</sup> which is unique to ortho-substituted benzyboronic acid viologens, and which stabilizes boronate ester formation, thus resulting in higher binding constants.

The differences in the fluorescence emission of HPTS with 4,4'-*o*-BBV (which cannot cooperatively bind glucose) versus that with 3,3'-*o*-BBV upon glucose addition are shown in Figure 5. These two receptors share in common the *o*-boronic acid positioning but differ in their quenching strengths. To balance out the quenching differences, a  $5 \times 10^{-4}$  M concentration of 3,3'-*o*-BBV was used to quench the fluorescence emission of HPTS (Figure 5a), while a lower concentration of 4,4'-*o*-BBV ( $2 \times 10^{-4}$  M) was used to achieve the same degree of quenching (Figure 5b). When each of these dye/quencher solutions was titrated with glucose, very different sensing profiles were obtained. The binding curve for 3,3'-*o*-BBV displays an early saturation and a slight sigmoidal shape,<sup>20</sup> whereas 4,4'-*o*-BBV gives a nearly linear response within the same glucose concentration range (Figure 5, insets).

To test for monosaccharide selectivity, the affinities of each of the BBVs for glucose, galactose, and fructose were compared (Table 3). The 4,4'-bipyridyl-based viologens (4,4'-*o*- and 4,4'-

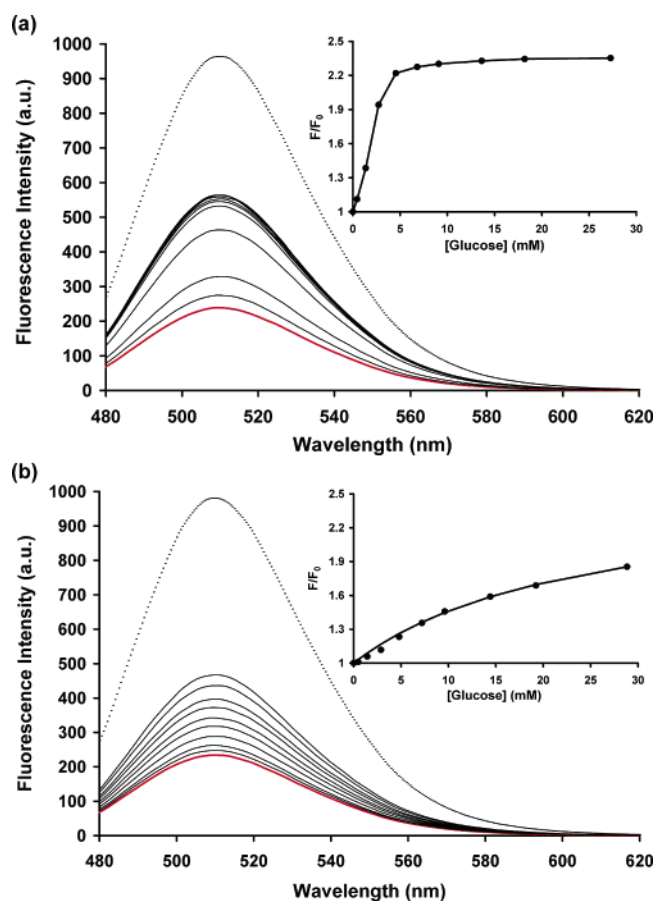


**Figure 5.** Change in fluorescence emission spectrum of HPTS ( $4 \times 10^{-6}$  M in pH 7.4 phosphate buffer,  $\lambda_{\text{ex}} = 460$  nm and  $\lambda_{\text{em}} = 510$  nm) in the presence of (a) 3,3'-*o*-BBV ( $5 \times 10^{-4}$  M), and (b) 4,4'-*o*-BBV ( $2 \times 10^{-4}$  M) upon addition of glucose. Dotted line = dye only, red line = dye and quencher, black lines = dye, quencher, and glucose. Insets are the binding isotherms: relative fluorescence increase ( $F/F_0$ ) of HPTS in the presence of quencher plotted as a function of glucose concentration.

*m*-BBV) exhibit saccharide selectivity of the order: fructose  $\gg$  galactose  $>$  glucose, where the fructose/glucose binding constant ratio is about 25:1 and the galactose/glucose ratio is about 1.5:1. As mentioned earlier, these ratios are similar to those obtained for monoboronic acids. The glucose selectivity of 3,3'-*m*-BBV and the 3,4'-bipyridyl-based viologens (3,4'-*o*- and 3,4'-*m*-BBV) were improved relative to that of the 4,4'-BBVs. These receptors display monosaccharide selectivity of the order fructose  $\gg$  glucose  $>$  galactose. The receptor 3,3'-*m*-BBV showed a slight preference for glucose over galactose (1.2:1), and a 10:1 preference for fructose over glucose. The selectivity ratios for 3,4'-*m*-BBV were a bit better, giving a 2:1 preference for glucose over galactose and a 6:1 preference for fructose over glucose. The receptor 3,4'-*o*-BBV was better still, displaying a 4:1 preference for glucose over galactose, and only a 3:1 preference for fructose over glucose.

Remarkably, 3,3'-*o*-BBV displayed an enhanced selectivity for glucose over fructose and galactose. For this receptor, the apparent binding constant for glucose is almost 2-fold higher than that of fructose, and 11-fold higher than that of galactose. It is important to note that, although the apparent binding constant of 3,3'-*o*-BBV was found to be higher for glucose than for fructose, the magnitude of fluorescence enhancement obtained upon addition of monosaccharide was greater for fructose.<sup>21</sup>

(19) All of the receptors were tested at this concentration. However, since the receptors have different quenching strengths and are used in molar excess relative to dye, the amount of the dye-receptor complex formed may vary for each receptor studied.

(20) (a) It is likely that the sigmoidal binding behavior may occur as a result of the large excess of [BBV] relative to that of [HPTS]; see: Metzger, A.; Anslyn, E. V. *Angew. Chem., Int. Ed.* **1998**, *37*, 649–652. (b) The [BBV]/[HPTS] ratio is large (125) for all the receptors studied, but the sigmoidal binding curve shape is most pronounced for 3,3'-*o*-BBV.

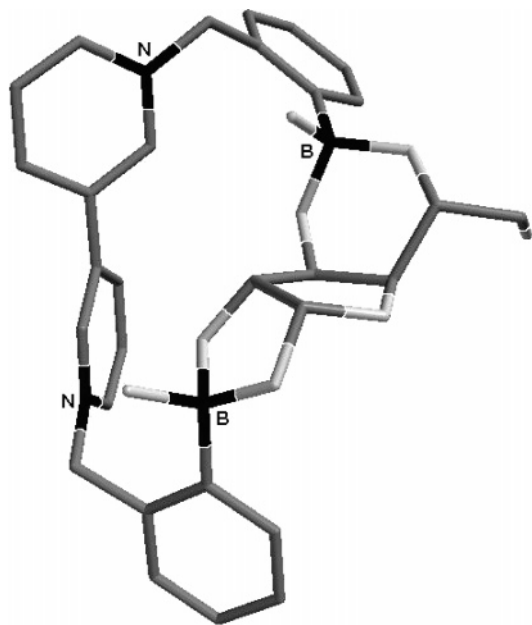


**Figure 6.** Energy-minimized structure of  $\alpha$ -D-glucofuranose-1,2:3,5-bisboronate of **3,3'-o-BBV** modeled in the gas phase (semiempirical AM1 using Spartan). Carbon atoms are in gray, and oxygen atoms are in white.

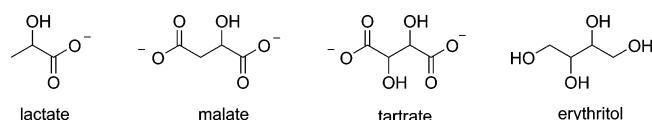


**Figure 7.** Structures of  $\alpha$ -hydroxycarboxylates and erythritol used in binding studies.

These fluorescence binding studies demonstrate the relatively exceptional glucose affinity of **3,3'-o-BBV** and suggest that this may be due to its ability to bind one glucose molecule through both boronic acid receptors. To verify that **3,3'-o-BBV** can indeed attain this type of binding mode without exorbitant energy expenditures relative to the unbound receptor, molecular modeling studies were performed. Although the form of glucose that predominates in solution is the  $\alpha$ -pyranose form, many studies aimed at structure elucidation of diboronic acid–glucose complexes reveal that the  $\alpha$ -furanose form is likely bound.<sup>22</sup> We thus modeled  $\alpha$ -glucopyranose bound to **3,3'-o-BBV** through the 1,2- and 3,5-hydroxyl groups (Figure 6).<sup>23</sup> A reasonable energy minimum was obtained for this structure, indicating its viability to form.

Finally, we studied the binding affinities of the BBVs for other analytes. In addition to *cis*-diols, boronic acids are also known to bind  $\alpha$ -hydroxy acids (at pH 7.4,  $\alpha$ -hydroxycarboxylates).<sup>24</sup> The BBVs were tested for their ability to bind lactate,

**Table 4.** Apparent Analyte Binding Constants ( $K_b$ ) Determined for the BBVs ( $5 \times 10^{-4}$  M) with HPTS ( $4 \times 10^{-6}$  M in Phosphate Buffer,  $\lambda_{\text{ex}} = 460$  nm and  $\lambda_{\text{em}} = 510$  nm) and Their Tartrate/Malate Selectivity Ratios.

	$K_b$ ( $\text{M}^{-1}$ )				selectivity ratio tartrate/malate
	tartrate	malate	lactate	erythritol	
<b>4,4'-o-</b>	$160 \pm 50$	$60 \pm 10$	$6 \pm 2$	$13 \pm 5$	2.7
<b>4,4'-m-</b>	$47 \pm 10$	$30 \pm 5$	$5 \pm 2$	$16 \pm 5$	1.6
<b>3,4'-o-</b>	$230 \pm 50$	$100 \pm 20$	$15 \pm 5$	$20 \pm 5$	2.3
<b>3,4'-m-</b>	$64 \pm 10$	$15 \pm 5$	$4 \pm 2$	$20 \pm 5$	4.3
<b>3,3'-o-</b>	$1250 \pm 100$	$160 \pm 50$	$26 \pm 5$	$38 \pm 10$	7.8
<b>3,3'-m-</b>	$250 \pm 50$	$60 \pm 10$	$18 \pm 5$	$34 \pm 5$	4.2

malate, tartrate, and erythritol (Figure 7). Erythritol, the diol counterpart of tartrate, was used to directly compare bis(diols) binding versus bis( $\alpha$ -hydroxycarboxylate) binding. The natural product tartaric acid is an optically active compound that is present in wine and other grape-based drinks. Some boronic acid-based sensors have been used to detect and quantify tartrate for possible applications in the beverage industry.<sup>25</sup> Chiral diboronic acid-based sensors have also been developed which are able to discriminate between L- and D-tartrate enantiomers.<sup>26</sup> Malic acid is structurally similar to tartaric acid and is also present in wine. Thus, the ability to distinguish between these two analytes is both useful and challenging. Lactate is present in the body, and its levels increase during exercise or when the body is under stress. When the body is at rest, the levels of lactic acid are about 1–2 mM. However, these levels can rise to 20 mM during intense physical exertion.

The calculated apparent binding constants for the  $\alpha$ -hydroxycarboxylates are shown in Table 4. Malate and tartrate both elicited large fluorescence increases (see Supporting Information) and moderate to high apparent binding constants with all the BBVs, whereas erythritol and lactate consistently produced weak fluorescence modulations and low binding constants. Comparing each BBV's selectivity ratio for tartrate and malate, **4,4'-o-**, **4,4'-m-**, and **3,4'-o-BBV** all have tartrate/malate binding constant ratios of about 2:1, while **3,3'-o-BBV** displays a ratio of 8:1. This suggests that **3,3'-o-BBV** may cooperatively bind tartrate. **3,4'-m-** and **3,3'-m-BBV** have tartrate/malate binding constant ratios of about 4:1. It is noteworthy the fact that all of the receptors displayed very low affinities for lactate—both in terms of binding constants and fluorescence signal enhancements. This is a desirable attribute for a clinical glucose sensor since the concentration of lactate in the blood can sometimes surpass that of glucose and could therefore interfere with glucose detection if the sensor was indiscriminate toward these two analytes.

## Conclusion

The signal transduction mechanism of this sensing system is based on the interaction between the viologen and HPTS. To

- (21) Other glucose sensing systems that display binding constants not proportional to changes in fluorescence intensities include: (a) Cao, H.; Diaz, D. I.; DiCesare, N.; Lakowicz, J. R.; Heagy, M. D. *Org. Lett.* **2002**, *4*, 1503–1505. (b) Gray, C. W., Jr.; Houston, T. A. *J. Org. Chem.* **2002**, *67*, 5426–5428. (c) Zhao, J.; Davidson, M. G.; Mahon, M. F.; Kociok-Koehn, G.; James, T. D. *J. Am. Chem. Soc.* **2004**, *126*, 16179–16186. (22) (a) Bielecki, M.; Eggert, H.; Norrild, J. C. *J. Chem. Soc., Perkin Trans. 2*, **1999**, 449–456. (b) Norrild, J. C.; Eggert, H. *J. Am. Chem. Soc.* **1995**, *117*, 1479–1484. (c) Eggert, H.; Frederiksen, J.; Morin, C.; Norrild, J. C. *J. Org. Chem.* **1999**, *64*, 3846–3852. (23) For completeness,  $\alpha$ -glucopyranose bound to **3,3'-o-BBV** and unbound **3,3'-o-BBV**, were also modeled and found to have similar minimized energies (see Supporting Information). (24) (a) Katzin, L. I.; Gulyas, E. *J. Am. Chem. Soc.* **1966**, *88*, 5209–5212. (b) Kustin, K.; Pizer, R. *J. Am. Chem. Soc.* **1969**, *91*, 317–322. (c) Friedman, S.; Pace, B.; Pizer, R. *J. Am. Chem. Soc.* **1974**, *96*, 5381–5384. (d) Friedman, S.; Pizer, R. *J. Am. Chem. Soc.* **1975**, *97*, 6059–6062.

- (25) (a) Lavigne, J. J.; Anslyn, E. V. *Angew. Chem., Int. Ed.* **1999**, *38*, 3666–3669. (b) Wiskur, S. L.; Ait-Haddou, H.; Lavigne, J. J.; Anslyn, E. V. *Acc. Chem. Res.* **2001**, *34*, 963–972. (c) Wiskur, S. L.; Floriano, P. N.; Anslyn, E. V.; McDevitt, J. T. *Angew. Chem., Int. Ed.* **2003**, *42*, 2070–2072. (d) Gray, C. W., Jr.; Houston, T. A. *J. Org. Chem.* **2002**, *67*, 5426–5428. (e) Manimala, J. C.; Wiskur, S. L.; Ellington, A. D.; Anslyn, E. V. *J. Am. Chem. Soc.* **2004**, *126*, 16515–16519. (f) Wiskur, S. L.; Lavigne, J. J.; Metzger, A.; Tobey, S. L.; Lynch, V.; Anslyn, E. V. *Chem. Eur. J.* **2004**, *10*, 3792–3804. (26) (a) Zhao, J.; Davidson, M. G.; Mahon, M. F.; Kociok-Koehn, G.; James, T. D. *J. Am. Chem. Soc.* **2004**, *126*, 16179–16186. (b) Zhao, J.; James, T. D. *Chem. Commun.* **2005**, 1889–1891. (c) Zhu, L.; Anslyn, E. V. *J. Am. Chem. Soc.* **2004**, *126*, 3676–3677. (d) Zhu, L.; Zhong, Z.; Anslyn, E. V. *J. Am. Chem. Soc.* **2005**, *127*, 4260–4269.

gain more insight into the nature of this interaction, a charge-transfer complex between **4,4'-*m*-BBV** and HPTS was formed in the solid state and studied by X-ray crystallography. This correlates with solution data, where evidence of a charge-transfer complex has been observed by UV-vis. Further elucidation of the viologen-HPTS interaction was accomplished via quenching studies. A relationship between Stern-Volmer quenching constants and the reduction potentials of benzyl viologens was established, which helped to confirm a donor-acceptor mechanism.

We have demonstrated that good analyte selectivity can be achieved by synthetically altering the viologen-based receptor unit to allow for cooperative binding of diboronic acids. The nitrogen-positioning in the bipyridyl rings, as well as the boronic acid-positioning around the benzyl rings, were modified in order to create receptors with unique binding environments relative to one another. One receptor, **3,3'-*o*-BBV**, displayed a very large binding constant for glucose and was found to be more selective for glucose over fructose. Other receptors showed selectivity for glucose over galactose and displayed enhanced glucose/fructose binding ratios. The six receptors were also screened against three different  $\alpha$ -hydroxycarboxylates in a neutral aqueous medium. Tartrate and malate both elicited large fluorescence increases and moderate to high apparent binding constants for all of the receptors. The receptor **3,3'-*o*-BBV**, displayed an 8-fold preference for tartrate over malate. Lactate, a potential interferent for in vivo glucose detection, was fortunately found to have very low binding constants with all of the receptors.

## Experimental Section

**Synthesis.** The syntheses of **4,4'-*o*-BBV**, **4,4'-*m*-BBV**, and **4,4'-*BV*** have been reported.<sup>9a</sup>

**General.** Reactions were performed using standard syringe techniques and were carried out in oven-dried glassware under an argon atmosphere. The 2- and 3-bromomethylphenylboronic acids were purchased from Lancaster. All other reagents were purchased from Aldrich. Dimethylformamide (DMF) was dried over CaH<sub>2</sub> prior to use. <sup>1</sup>H NMR spectra were recorded on a Varian spectrometer at 500 MHz and are reported in ppm with respect to TMS ( $\delta = 0$ ). Proton decoupled <sup>13</sup>C NMR spectra were recorded on a Varian at 125 MHz and are reported in ppm.<sup>27</sup> <sup>11</sup>B NMR spectra were recorded on a Bruker at 80.25 MHz and are reported in ppm with respect to BF<sub>3</sub>·OEt<sub>2</sub> ( $\delta = 0$ ). High-resolution mass measurements were obtained on a benchtop Mariner ESITOF mass spectrometer or a JEOL JMS-AX505HA mass spectrometer from a matrix of *p*-nitrobenzyl alcohol for FAB.

**3,4'-Bipyridyl (3).** To a 100-mL oven-dried round-bottomed flask with a sidearm and condenser, was added 3-bromopyridine (1.16 mL, 12 mmol), 4-pyridineboronic acid (1.23 g, 10 mmol), and anhydrous 1,4-dioxane (20 mL) under argon. A degassed aqueous solution of Na<sub>2</sub>CO<sub>3</sub> (2 M, 10 mL) was then added via syringe to the vigorously stirred reaction mixture, followed by the addition of Pd(OAc)<sub>2</sub> (0.11 g, 0.5 mmol) and PPh<sub>3</sub> (0.65 g, 2.5 mmol). The reaction flask was then purged by using five argon/vacuum back-fill cycles and then stirred for 4 h at 95 °C. After cooling to room temperature, water was added (50 mL), and the reaction was extracted with ethyl acetate (2 × 100 mL). The combined organics were washed with brine (2 × 75 mL), dried with MgSO<sub>4</sub>, and evaporated to an oil under reduced pressure. The residue was purified by chromatography on silica gel (pretreated with 10% triethylamine in dichloromethane) using 1:1 ethyl acetate/dichloromethane to give 1.1 g (70% yield) of clear oil. Spectroscopic data

were in accord with those previously reported.<sup>28</sup> <sup>1</sup>H NMR (CDCl<sub>3</sub>, 500 MHz)  $\delta$  7.15 (ddd,  $J = 7.75, 4.5, 1.0$  Hz, 1H), 7.24 (dd,  $J = 4.5, 1.5$  Hz, 2H), 7.66 (dt,  $J = 8.0, 2.0$  Hz, 1H), 8.41 (dd,  $J = 5.0, 1.5$  Hz, 1H), 8.44 (d,  $J = 4.5, 1.5$  Hz, 2H), 8.63 (d,  $J = 1.5, 1$  Hz); <sup>13</sup>C NMR (CDCl<sub>3</sub>, 125 MHz)  $\delta$  121.4, 123.7, 133.5, 134.2, 144.9, 148.0, 150.0, 150.4.

***N,N'*-Bis-(benzyl-2-boronic acid)-[3,4']bipyridinium Dibromide (3,4'-*o*-BBV).** To a solution of 2-bromomethylphenylboronic acid (0.3 g, 1.38 mmol) in DMF (15 mL) was added 3,4'-bipyridyl (0.095 g, 0.6 mmol), and the reaction was stirred at 70 °C for 48 h. After the mixture cooled to room temperature, acetone (50 mL) was added to the clear yellow solution. The resulting pale-yellow precipitate was collected by centrifugation, washed with acetone, and dried under a stream of argon (0.27 g, 77% yield). <sup>1</sup>H NMR (D<sub>2</sub>O, 500 MHz)  $\delta$  6.21 (s, 2H), 6.27 (s, 2H), 7.71 (m, 6H), 7.92 (m, 2H), 8.39 (dd,  $J = 8.5, 6.5$  Hz, 1H), 8.51 (d,  $J = 6.5$  Hz, 2H), 9.16 (m, 4H), 9.60 (s, 1H); <sup>13</sup>C NMR (D<sub>2</sub>O, 62.5 MHz)  $\delta$  66.0, 66.7, 127.4, 130.0, 130.9, 131.0, 132.3, 132.3, 132.5, 132.7, 136.2, 136.3, 136.3, 136.7, 136.8, 145.3, 146.2, 146.9, 147.5, 150.9; <sup>11</sup>B NMR (80 MHz, D<sub>2</sub>O)  $\delta$  28.3. HRMS-ESI  $m/z$  calcd for C<sub>24</sub>H<sub>24</sub>B<sub>2</sub>BrN<sub>2</sub>O<sub>4</sub> [M - Br]<sup>+</sup>: 505.11056, found 505.11693.

***N,N'*-Bis-(benzyl-3-boronic acid)-[3,4']bipyridinium Dibromide (3,4'-*m*-BBV).** To a solution of 3-bromomethylphenylboronic acid (0.69 g, 3.2 mmol) in DMF (25 mL) was added 3,4'-bipyridyl (0.2 g, 1.28 mmol), and the reaction was stirred at 80 °C for 48 h. The yellow precipitate was collected by centrifugation, washed with DMF and then acetone, and dried under a stream of argon (0.58 g, 76% yield). <sup>1</sup>H NMR (D<sub>2</sub>O, 500 MHz)  $\delta$  6.04 (s, 2H), 6.09 (s, 2H), 7.65 (q,  $J = 7.5$  Hz, 2H), 7.73 (d,  $J = 7.5$  Hz, 2H), 7.95 (m, 4H), 8.40 (dd,  $J = 8.0, 6.5$  Hz, 1H), 8.55 (d,  $J = 7.0$  Hz, 2H), 9.13 (d,  $J = 8.5$  Hz, 1H), 9.23 (m, 3H), 9.65 (s, 1H); <sup>13</sup>C NMR (D<sub>2</sub>O, 125 MHz)  $\delta$  66.0, 66.6, 127.9, 130.4, 130.5, 132.8, 132.9, 133.1, 133.2, 135.6, 135.6, 136.5, 136.5, 136.6, 145.2, 146.4, 146.7, 147.4, 151.0; <sup>11</sup>B NMR (80 MHz, D<sub>2</sub>O)  $\delta$  24.8. HRMS-ESI  $m/z$  calcd for C<sub>24</sub>H<sub>24</sub>B<sub>2</sub>BrN<sub>2</sub>O<sub>4</sub> [M - Br]<sup>+</sup>: 505.11056, found 505.10820.

**3,3'-Bipyridyl (2).** To a 100-mL oven-dried round-bottomed flask with a sidearm and condenser, was added 3-bromopyridine (1.16 mL, 12 mmol), 3-pyridineboronic acid (1.23 g, 10 mmol), and anhydrous 1,4-dioxane (20 mL) under argon. A degassed aqueous solution of Na<sub>2</sub>CO<sub>3</sub> (2 M, 10 mL) was then added via syringe to the vigorously stirred reaction mixture, followed by the addition of Pd(OAc)<sub>2</sub> (0.11 g, 0.5 mmol) and PPh<sub>3</sub> (0.65 g, 2.5 mmol). The reaction flask was then purged using five argon/vacuum back-fill cycles, then stirred for 2 h at 95 °C. After the mixture was cooled to room temperature, water was added (50 mL), and the reaction was extracted with ethyl acetate (2 × 100 mL). The combined organics were washed with brine (2 × 75 mL), dried with MgSO<sub>4</sub>, and evaporated to an oil under reduced pressure. The residue was purified by chromatography on silica gel (pretreated with 10% triethylamine in dichloromethane) using 20% ethyl acetate in dichloromethane to give 1.0 g (64% yield) of clear oil. Spectroscopic data were in accord with those previously reported.<sup>29</sup> <sup>1</sup>H NMR (CDCl<sub>3</sub>, 500 MHz)  $\delta$  7.38 (dd,  $J = 8.0, 5.0$  Hz, 2H), 7.86 (dt,  $J = 7.5, 2.0$  Hz, 2H), 8.62 (dd,  $J = 5.0, 1.5$  Hz, 2H), 8.81 (d,  $J = 2.5$  Hz, 2H); <sup>13</sup>C NMR (CDCl<sub>3</sub>, 125 MHz)  $\delta$  123.9, 133.6, 134.5, 148.3, 149.4.

***N,N'*-Bis-(benzyl-2-boronic acid)-[3,3']bipyridinium Dibromide (3,3'-*o*-BBV).** To a solution of 2-bromomethylphenylboronic acid (0.59 g, 2.76 mmol) in DMF (20 mL) was added 3,3'-bipyridyl (0.187 g, 1.2 mmol), and the reaction was stirred at 70 °C for 48 h. After the mixture was cooled to room temperature, acetone (50 mL) was added to the clear yellow solution. The resulting white precipitate was collected by centrifugation, washed with acetone, and dried under a stream of argon (0.56 g, 80% yield). <sup>1</sup>H NMR (D<sub>2</sub>O, 500 MHz)  $\delta$  6.20 (s, 4H), 7.68 (m, 6H), 7.90 (d,  $J = 7.0$  Hz, 2H), 8.34 (dd,  $J = 8.5, 6.5$  Hz, 2H), 8.95 (d,  $J = 8.0$  Hz, 2H), 9.14 (d,  $J = 6.5$  Hz, 2H), 9.27 (s, 2H); <sup>13</sup>C NMR

(27) Due to relaxed <sup>13</sup>C-<sup>11</sup>B spin-spin coupling, signals for carbons directly attached to boron are not observed.

(28) Shiao, M. J.; Shieh, P.; Lai, J. S. *Synth. Commun.* **1988**, *18*, 1397-1402.

(29) Fort, Y.; Becker, S.; Caubere, P. *Tetrahedron* **1994**, *50*, 11893-11902.



(D<sub>2</sub>O, 62.5 MHz)  $\delta$  65.2, 128.5, 129.7, 131.0, 131.3, 134.2, 135.0, 135.3, 143.2, 144.6, 145.4; <sup>11</sup>B NMR (80 MHz, D<sub>2</sub>O)  $\delta$  28.7. HRMS-ESI  $m/z$  calcd for C<sub>24</sub>H<sub>24</sub>B<sub>2</sub>BrN<sub>2</sub>O<sub>4</sub> [M – Br]<sup>+</sup>: 505.11056, found 505.10291.

***N,N'*-Bis-(benzyl-3-boronic acid)-[3,3']bipyridinium Dibromide (3,3'-*m*-BBV).** To a solution of 3-bromomethylphenylboronic acid (0.69 g, 3.2 mmol) in DMF (25 mL) was added 3,3'-bipyridyl (0.2 g, 1.28 mmol), and the reaction was stirred at 80 °C for 48 h. The white precipitate was collected by centrifugation, washed with DMF and then acetone, and dried under a stream of argon (0.57 g, 76% yield). <sup>1</sup>H NMR (D<sub>2</sub>O, 500 MHz)  $\delta$  6.04 (s, 4H), 7.59 (t, *J* = 7.5 Hz, 2H), 7.69 (d, *J* = 8.5 Hz, 2H), 7.87 (d, *J* = 7.5 Hz, 2H), 7.90 (s, 2H), 8.37 (dd, *J* = 7.5, 6.0 Hz, 2H), 9.0 (d, *J* = 8.0 Hz, 2H), 9.2 (d, *J* = 6.0 Hz, 2H), 9.45 (s, 2H); <sup>13</sup>C NMR (D<sub>2</sub>O, 125 MHz)  $\delta$  66.5, 130.4, 130.5, 133.0, 135.1, 135.7, 135.8, 136.6, 144.5, 146.2, 146.6; <sup>11</sup>B NMR (80 MHz, D<sub>2</sub>O)  $\delta$  26.0. HRMS-ESI  $m/z$  calcd for C<sub>24</sub>H<sub>24</sub>B<sub>2</sub>BrN<sub>2</sub>O<sub>4</sub> [M – Br]<sup>+</sup>: 505.11056, found 505.10969.

***N,N'*-3,4'-Bis(benzyl)bipyridinium Dibromide (3,4'-BV).** To a solution of benzyl bromide (0.45 mL, 3.75 mmol) in DMF (5 mL) was added 3,4'-bipyridyl (0.23 g, 1.5 mmol), and the reaction was stirred at 70 °C for 16 h. The yellow precipitate was collected by centrifugation, washed with acetone, and dried under a stream of argon (0.67 g, 90% yield). <sup>1</sup>H NMR (D<sub>2</sub>O, 500 MHz)  $\delta$  6.08 (s, 2H), 6.14 (s, 2H), 7.69 (m, 10H), 8.47 (dd, *J* = 8.0, 6.0 Hz, 1H), 8.62 (d, *J* = 7.0 Hz, 2H), 9.21 (dt, *J* = 8.0, 2.0 Hz, 1H), 9.28 (d, *J* = 7.0 Hz, 2H), 9.29 (m, 1H), 9.71 (s, 1H); <sup>13</sup>C NMR (D<sub>2</sub>O, 62.5 MHz)  $\delta$  66.0, 66.6, 128.0, 130.5, 130.7, 130.8, 131.1, 131.5, 131.6, 133.5, 133.6, 136.5, 145.2, 146.5, 146.7, 147.4, 150.9. HRMS-FAB  $m/z$  calcd for C<sub>24</sub>H<sub>22</sub>BrN<sub>2</sub> [M – Br]<sup>+</sup>: 417.0966, found 417.1004.

***N,N'*-3,3'-Bis(benzyl)bipyridinium Dibromide (3,3'-BV).** To a solution of benzyl bromide (0.45 mL, 3.75 mmol) in DMF (5 mL) was added 3,3'-bipyridyl (0.23 g, 1.5 mmol), and the reaction was stirred at 70 °C for 16 h. The yellow precipitate was collected by centrifugation, washed with acetone, and dried under a stream of argon (0.67 g, 90% yield). <sup>1</sup>H NMR (D<sub>2</sub>O, 500 MHz)  $\delta$  6.12 (s, 4H), 7.70 (m, 10H), 8.45 (dd, *J* = 8.0, 6.0 Hz, 2H), 9.07 (dt, *J* = 8.0, 1.5 Hz, 2H), 9.27 (d, *J* = 6.0 Hz, 2H), 9.55 (s, 2H); <sup>13</sup>C NMR (D<sub>2</sub>O, 62.5 MHz)  $\delta$  66.6, 130.4, 130.8, 131.1, 131.6, 133.5, 135.9, 144.6, 146.2, 146.6. HRMS-FAB  $m/z$  calcd for C<sub>24</sub>H<sub>22</sub>BrN<sub>2</sub> [M – Br]<sup>+</sup>: 417.0966, found 417.0956.

**Cyclic Voltammetry.** Cyclic voltammetry was performed on CHI 440 electrochemical workstation. A glassy carbon (GC) working electrode (polished using METASERV 2000 Polisher/Grinder), a Ag/AgCl reference electrode, and a platinum wire as counter electrode were used as a normal three-electrode configuration. Potentials were reported against the normal hydrogen electrode (NHE). The test solution, containing 5 mM viologen in pH 7.4 phosphate buffer (0.1 M ionic strength), was purged with argon, and a stream of argon was maintained above it to keep the solution anaerobic.

**X-ray Structure Determination.** (BBV<sup>2+</sup>)<sub>3</sub>(HPTS<sup>3-</sup>)<sub>2</sub>·2CH<sub>3</sub>·OH·2H<sub>2</sub>O. A concentrated aqueous solution of 4,4'-*m*-BBV (1 mL) was added to a concentrated aqueous solution of HPTS (1 mL), resulting in immediate precipitation of a fluffy, pink solid. The solid was then isolated and dissolved in hot methanol/water (10:1). After standing at room temperature for 3 days, dark-red colored crystals formed.

A needle of dimensions 0.02 × 0.25 × 0.38 mm<sup>3</sup> was mounted in the 93(2) K nitrogen cold stream provided by a CRYO Industries low temperature apparatus on the goniometer head of a Bruker SMART Apex diffractometer equipped with an ApexII CCD detector. Diffraction data were collected with graphite-monochromated Mo K $\alpha$  radiation employing a 0.3°  $\omega$  scans and approximately a full sphere of data to 2 $\theta_{\max}$  of 55°. A multiscan correction for absorption was applied using the program SADABS 2.10. Upon inspection of the scattering intensities the data were truncated to 2 $\theta$  = 53°, yielding a total of 26407 reflections

collected, of which 10432 were unique [ $R(\text{int})$  = 0.1020], and 5162 were observed [ $I > 2\sigma(I)$ ]. The structure was solved by direct methods (SHELXS-97) and refined by full-matrix least-squares on  $F^2$  (SHELXL97) using 761 parameters. All non-hydrogen atoms were refined with anisotropic thermal parameters. The H atoms on C atoms were generated geometrically and refined as riding atoms with C–H = 0.95–0.99 Å and Uiso(H) = 1.2 times Ueq(C) for CH, CH<sub>2</sub> and OH groups, Uiso(H) = 1.5 times Ueq(C) for CH<sub>3</sub> groups. The H atoms on O atoms were found in the electron difference map and refined as riding atoms with O–H = 0.86 Å and Uiso(H) = 1.2 times Ueq(O). The maximum and minimum peaks in the final difference Fourier map were 0.805 and –0.429 e Å<sup>–3</sup>. Crystal Data: C<sub>108</sub>H<sub>102</sub>B<sub>6</sub>N<sub>6</sub>O<sub>36</sub>S<sub>6</sub>, MW = 2317.18, triclinic,  $P\bar{1}$ ,  $a$  = 9.5930(12) Å,  $b$  = 13.9110(17) Å,  $c$  = 20.342(2) Å,  $\alpha$  = 102.126(2)°,  $\beta$  = 90.323(2)°,  $\gamma$  = 105.605(2)°.  $V$  = 2550.6(5) Å<sup>3</sup>,  $T$  = 93(2) K,  $Z$  = 1,  $R_1$  [ $I > 2\sigma(I)$ ] = 0.0629,  $wR_2$  (all data) = 0.1810, GOF (on  $F^2$ ) = 0.981.

**Fluorescence Measurements. General.** All reagents and analytes were purchased from Aldrich. All solutions were prepared with water that was purified via a Barnstead NANOpure system (17.7 MΩ/cm). Buffers (pH 7.4, 0.1 ionic strength) were freshly prepared from KH<sub>2</sub>PO<sub>4</sub> and Na<sub>2</sub>HPO<sub>4</sub> before use. pH measurements were taken on a Denver Instrument UB-10 pH/mV meter and calibrated with standard buffer solutions (pH 4, 7, and 10 from Fisher). Fluorescence spectra were taken on a Perkin-Elmer LS50-B luminescence spectrometer, and were carried out at 25 °C. Standard quartz fluorescence cuvettes were used in all studies. HPTS was excited at 460 nm, and the emission ( $\lambda_{\max}$  = 510 nm) was collected from 480 to 650 nm. All experiments were carried out in triplicate, and the errors in the reported binding constants are based on the standard deviation of three independent determinations. All data were analyzed using the Solver (nonlinear least-squares curve fitting) in Microsoft Excel.

**Fluorescence Measurements for Quenching Studies.** Fluorescence measurements were done in situ by taking the emission spectrum of HPTS at a series of quencher concentrations. The emission spectrum of HPTS (2 mL of 4 × 10<sup>–6</sup> M in buffer) was first obtained, quencher was added (0.5–10  $\mu$ L aliquots of 5 mM in buffer), the solution was shaken for 30 s, and the new emission was measured after each quencher addition.

**Data Analysis.** Stern–Volmer quenching constants were calculated by fitting the data with eq 1:

$$F_0/F = (1 + K_s[Q])e^{V[Q]} \quad (1)$$

where  $F_0$  is the initial fluorescence intensity,  $F$  is the fluorescence intensity after the addition of quencher,  $V$  is the dynamic quenching constant,  $K_s$  is the static quenching constant, and  $[Q]$  is the quencher concentration.<sup>13d</sup>

**Fluorescence Measurements for Analyte Sensing Studies.** The emission spectrum of HPTS (2 mL of 4 × 10<sup>–6</sup> M in buffer) was taken, quencher was added (200  $\mu$ L of 5 mM in buffer) to obtain a quencher/HPTS ratio of 125:1, the emission measured, and then analyte solution was added (0.5–10  $\mu$ L aliquots of 1 M in pH 7.4 buffer); the solution was shaken for 30 s, and the new emission was measured after each addition of analyte.

**Data Analysis.** Apparent binding constants were calculated by fitting the data with eq 2:

$$F/F_0 = (1 + (F_{\max}/F_0)K_b[A])/(1 + K_b[A]) \quad (2)$$

where  $F_0$  is the fluorescence intensity of the quenched dye,  $F$  is the fluorescence intensity after the addition of analyte,  $F_{\max}$  is the calculated intensity at which the fluorescence reaches its maximum,  $K_b$  is the apparent binding constant, and  $[A]$  is the concentration of analyte.<sup>30</sup>

**Acknowledgment.** The authors thank the BioSTAR Project and the Industry-University Cooperative Research Program with

(30) Cooper, C. R.; James, T. D. *J. Chem. Soc., Perkin Trans. 1* **2000**, 963–969.



GluMetrics, Inc. for their financial support. We also thank Professor Shaowei Chen for his helpful discussions.

**Supporting Information Available:** Fluorescence spectra, binding isotherms, cyclic voltammograms, molecular modeling

coordinates,  $^1\text{H}$  and  $^{13}\text{C}$  NMR spectra for all compounds reported; crystallographic information files (CIF). This material is available free of charge via the Internet at <http://pubs.acs.org>.

JA066567I